Journal of Inorganic and General Chemistry

ZAAC
Zeitschrift für anorganische und allgemeine Chemie

www.zaac.wiley-vch.de

RESEARCH ARTICLE

Check for updates

Special Collection

[(K,Rb)@([2.2.2]crypt)]$_2$(K,Rb)$_4$[Si$_9$W(CO)$_4$]·13.4 NH$_3$ – The First Tungsten Functionalized Silicon Zintl Cluster

Paul A. Braun,[a] Franz F. Westermair,[b] Ruth M. Gschwind,[b] and Nikolaus Korber*[a]

On the occasion of the 125th birthday of Prof. Dr. Eduard Zintl.

The reaction between the heteroleptic metal carbonyl complex [W(CO)$_4$(tmeda)] ((tmeda)=*N,N,N′,N′*-Tetramethylethane-1,2-diamine) with [Si$_9$]$^{4-}$ silicon Zintl clusters in presence of [2.2.2]crypt ([2.2.2]crypt=4,7,13,16,21,24-Hexaoxa-1,10-diazabicyclo[8.8.8]-hexacosane) in liquid ammonia yielded the compound [(K,Rb)@-([2.2.2]crypt)]$_2$(K,Rb)$_4$[Si$_9$W(CO)$_4$]·13.4 NH$_3$. The compound was analyzed by single crystal X-ray diffraction and crystallizes in the space group $P\bar{1}$ (a=11.48390(10) Å, b=19.7383(2) Å, c=19.8983(2) Å, α=112.5760(10)°, β=97.4210(10)°, γ= 95.3760(10)°, V=4079.01(7) Å^3). The compound represents the first group 6 carbonylate-functionalized silicon Zintl cluster. The central moiety is composed of a tricapped trigonal prismatic nine-atom silicon species which coordinates with the lone pair of one capping atom to the tungsten tetracarbonylate, forming a pseudo trigonal bipyramidal carbonylate cluster anion [Si$_9$W-(CO)$_4$]$^{6-}$. The chemical bonding in the new cluster entity is analyzed using theoretical calculations and subsequent analysis using QTAIM and NBO.

Introduction

The highly charged group 14 Zintl ions are a topic of research since their discovery by *Joannis* in 1891.[1] Especially the cluster anions of the lighter group 14 elements silicon and germanium are interesting in terms of materials science.[2] *Fässler et al.* recently published a paper investigating the quantum chemical mixing behavior of Si and Ge within (Si$_{9-x}$Ge$_x$)$^{4-}$ (x=0, 1, 2) Zintl anions.[3] A current focus in research is set on the derivatization of these molecular building blocks with silanes and/or transition metal complexes.[4,5] Two families of organometallic reagents which yield a large variety of interesting, functionalized clusters are NHC (N-heterocyclic carbene) metal complexes and metal carbonyl complexes.[6] Since the homoleptic carbonyl complexes hardly show any reactivity towards the Zintl clusters, labile ligands like mesitylene, toluene, PPh$_3$, etc. were

introduced.[7] The reactions with heteroleptic complexes like e.g. [Cr(CO)$_3$·(tol)], [Mo(CO)$_3$(MeCN)$_3$] and [M(CO)$_3$(mes)] (M=Cr, Mo, W; mes=η^6-1,3,5-C$_6$Me$_3$H$_3$) resulted in the first metal carbonyl-functionalized Zintl clusters: [Sn$_9$M(CO)$_3$]$^{4-}$ and [Pb$_9$M-(CO)$_3$]$^{4-}$ (M=Cr, Mo, W).[8,9,10] The transition metals typically tetra-coordinate the square plane of the monocapped square antiprismatic cluster, and even new clusters involving the {M(CO)$_3$} fragment in a penta-coordination can be observed.[9,10] A few years later the group 6 metal carbonyl functionalization of germanium clusters could be achieved *via* a gas phase deposition route, leading to the characterization of [Ge$_9$(Si-(SiMe$_3$)$_3$M(CO)$_3$]$^-$ (M=Cr, Mo, W) and [Ge$_9$(Si(SiMe$_3$)$_3$Cr(CO)$_5$]$^-$.[11]

Also to mention is the chemistry of group 15 Zintl clusters with group 6 transition metal carbonyls which results in a wide variety of functionalized clusters like [E$_7$M(CO)$_3$]$^{3-}$ (E=P, As, Sb, M=Cr, Mo, W), [Bi$_3$M$_2$(CO)$_6$]$^{3-}$ (M=Cr, Mo), [Bi$_6$Mo$_3$(CO)$_9$]$^{4-}$ and [η^3-Bi$_3$W(CO)$_3$]$^{3-}$.[5,7,12]

Especially for germanium, a multitude of different structure motifs is known. For group 6 there are further examples like [Ge$_9${M(CO)$_5$}$_3$]$^{4-}$ (M=Cr, Mo, W) with the {M(CO)$_5$} fragments coordinating the three capping Ge atoms of the nine atom cluster in its tricapped prismatic shape.[13] Further examples for transition-metal-carbonyl-functionalized germanium clusters are [Ge$_8${Mo(CO)$_3$}$_2$]$^{4-}$ with a intermolecular Mo—Mo interaction, [{(CO)$_5$M}$_6$Tt$_6$]$^{2-}$ (M=Cr, Mo, W; Tt=Ge, Sn) as an derivative of the unknown [Ge$_6$]$^{2-}$ anion,[14] and [Ge$_{10}$Mn(CO)$_4$]$^{3-}$.[15] Very recently also the cluster [(CrGe$_9$)Cr$_2$(CO)$_{13}$]$^{4-}$ was published showing a combination of a penta- and mono-coordination of the carbonyl fragment.[16] Outside of group 6, the anion [Ge$_8$Fe(CO)$_3$]$^{3-}$ was reported with a replaced vertex of a [Ge$_9$]$^{4-}$ cluster.[17] Notable is also [Ge$_5$Ni$_2$(CO)$_3$]$^{2-}$ which shows a functionalized [Ge$_5$]$^{2-}$ anion.[18] The reaction of germanium or tin Zintl ions with [Ni(CO)$_2$(PPh$_3$)$_2$] even results in endohedral or fused clusters. Examples for Ni functionalized clusters are [Ni@Sn$_9$Ni(CO)]$^{3-}$, [Ni$_6$Ge$_{13}$(CO)$_5$]$^{4-}$, [Co@Sn$_9$Ni(CO)]$^{3-}$ and

[a] P. A. Braun, Prof. Dr. N. Korber
Institute of Inorganic Chemistry
University of Regensburg
93040 Regensburg, Germany
E-mail: nikolaus.korber@ur.de
[b] F. F. Westermair, Prof. Dr. R. M. Gschwind
Institute of Organic Chemistry
University of Regensburg
93040 Regensburg, Germany

Special Collection
This article is part of a Special Collection to celebrate Professor Eduard Zintl on the occasion of his 125th anniversary. Please see our homepage for more articles in the collection.

$[Sn_5Ni_6(CO)_9]^{4-}$.[19] In contrast to the rich coordination chemistry of germanium clusters, for bare silicon clusters, only few transition-metal-coordinated clusters have been reported to date. The first structure $[Si_9ZnPh]^{3-}$ was published by *Sevov* et al. in 2006.[20] Since then, additions were $[(MesCu)_2Si_4]^{4-}$, $[(NHC^{tBu}Au)_6(\eta^2\text{-}Si_4)]^{2+}$, $[NHC^{Dipp}Cu(\eta^4\text{-}Si_9)]^{3-}$ and $[\{Ni(CO)_2\}_2(\mu\text{-}Si_9)_2]^{8-}$.[21,22] The latter represents the first metal-carbonyl-coordinated silicon cluster.

In general, solution studies in liquid ammonia by NMR spectroscopy provide the possibility of further investigation of silicon clusters by ^{1}H- and ^{29}Si-NMR. In past experiments, the protonated silicon Zintl anions $[HSi_9]^{3-}$, $[H_2Si_9]^{2-}$ and $[HSi_4]^{3-}$ could be detected.[23,24] Recently, NMR spectroscopy allowed for the detection of the first protonated group 14 Zintl cluster coordinating to a coinage metal, the existence of $[NHC^{Dipp}Cu(\eta^4\text{-}Si_9)H]^{2-}$ was supported by crystallographic data and computational analyses.[25]

We here report on the synthesis and characterisation of the first tungsten-functionalized silicon cluster anion $[Si_9W(CO)_4]^{6-}$ in the ammoniate $[(K,Rb)@([2.2.2]crypt)]_2(K,Rb)_4[Si_9W(CO)_4]\cdot 13.4$ NH_3.

Results and Discussion

Crystal Structure of $[(K,Rb)@([2.2.2]crypt)]_2(K,Rb)_4$ $[Si_9W(CO)_4]\cdot 13.4\ NH_3$

The reaction of $K_6Rb_6Si_{17}$ with $W(CO)_4(tmeda)$ in the presence of [2.2.2]crypt in liquid ammonia resulted in crystals of the compound $[(K,Rb)@([2.2.2]crypt)]_2(K,Rb)_4[Si_9W(CO)_4]\cdot 13.4$ NH_3. The central moiety is represented by a $[Si_9]^{4-}$ cluster which coordinates via one vertex silicon atom to the tungsten tetracarbonylate $[W(CO)_4]^{2-}$. The resulting complex $[Si_9W(CO)_4]^{6-}$ is directly coordinated by four alkali metal cations (A = K, Rb). The two remaining cations are found in the cavity of [2.2.2]cryptands. Therefore, the overall charge of the anion sums up to −6.

The shape of this type of nine atom clusters can be evaluated using the h/e ratio (ideally h/e = 1 for the tricapped prism with point group D_{3h}) or the d1/d2 ratio (ideally d1/d2 = 1 for the monocapped square antiprism with the point group C_{4v}).[26] For the silicon cluster in $[Si_9W(CO)_4]^{6-}$ (Figure 1), a h/e ratio of 1.19 and a d1/d2 ratio of 1.39 is determined. An unequivocal assignment of the cluster symmetry is therefore not possible. The Si–Si distances range from 2.4328(18) Å to 3.191(2) Å, which corresponds well to literature values.[27]

The tungsten tetracarbonlyate fragment shows W–C distances in the range of 1.934(6) Å to 1.978(5) Å and C–O bonds in the range of 1.156(6) Å to 1.219(7) Å, which are both in agreement with the literature.[28,29] The CO group opposite to the $[Si_9]^{4-}$ cage shows a slightly prolonged W–C4 distance (1.978(5) Å) and accordingly shortened C4–O4 bond (1.156(6) Å). The W–Si1 distance is 2.6649(13) Å which fits well into the range of other W–Si distances.[30] The equatorial C1O1, C2O2 and C3O3 groups show (∡C–W–C) angles of 118.3(2)° to 121.7(3)°, the apical to equatorial (∡C4–W–Cx, x = 1–3) angles
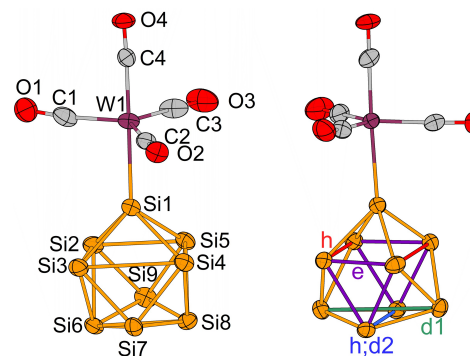
Figure 1. Asymmetric unit of the central moiety $[Si_9W(CO)_4]^{6-}$ in $[(K,Rb)@([2.2.2]crypt)]_2(K,Rb)_4[Si_9W(CO)_4]\cdot 13.4\ NH_3$ and representation of the d1/d2 diagonals and h/e bonds. The displacement ellipsoids are shown at 50 % probability.

are 84.12(15)° to 92.37(16)°, and the apical to apical (∡C4–W–Si1) angle is 177.40(15)°. The structure can be compared to the structurally related metal pentacarbonylates which also preferentially form a trigonal bipyramid.[28,31]

The chelated alkali metal positions A5 (=K5/Rb5) and A6 (= K5/Rb5) can be resolved as 91.5/8.5 % and 91.0/9.0 % K/Rb. A refinement model with fully occupied potassium resulted in significantly larger residual electron density (Figure SI3), which indicated the additional presence of a heavier alkali metal cation at this position. The non-chelated alkali metal positions (Figure 2) K1/Rb1 (=A1, 46.6/53.4 %), K2/Rb2 (=A2, 31.8/ 68.2 %), K3/Rb3 (=A3, 69.9/30.1 %) and K4/Rb4 (=A4, 29.8/ 70.2 %) are coordinated to the cluster. These four directly coordinating cations are instrumental for the stabilization of the unusually high charge of the cluster anion. The position of A1 additionally coordinates a triangular face of a second Si_9 cage,
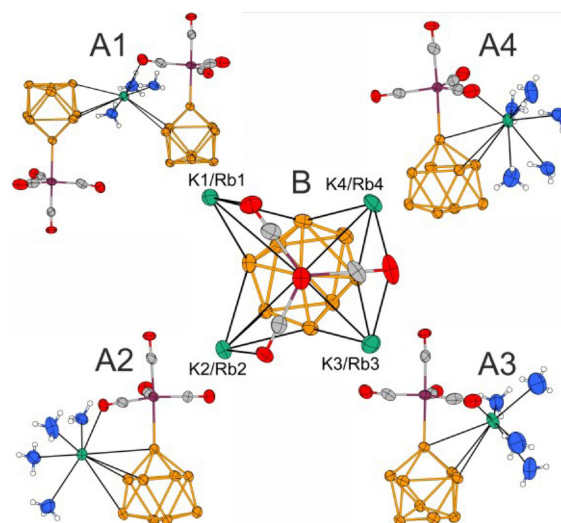

Figure 2. Alkali metal vicinity of the anion surrounding cations (**B**) and the coordination spheres of alkali metal position **A1** (K/Rb: 46.6/53.4 %), **A2** (31.8/68.2 %), **A3** (69.9/30.1 %) and **A4** (29.8/70.2 %). The displacement ellipsoids are shown at 50 % probability.

A2 is coordinated by four silicon atoms of the nonasilicide anion, A3 and A4 cap triangular faces of the Si_9 unit. The observed A–Si distances range from 3.4863(18) Å to 4.1783(18) Å, which is in accordance with literature.[27] Additionally, the alkali metals are coordinated by one oxygen atom of the respective carbonyl groups at A–O distances from 2.725(6) Å to 3.089(4) Å, which are within the expected range.[21]

The coordination spheres of the positions A2–A4 are completed by ammonia molecules of solvation (A1: 3×NH_3; A2: A2/A3 4×NH_3; A4: 5×NH_3). This results in a coordination number of nine for A1/A2/A4 and eight for A3. This in turn corresponds to the alkali metal occupation, as the larger rubidium cation is predominantly present at A1/A2/A4, while the smaller volume of A3 favours the occupation by potassium. Regarding direct cation-anion interactions, $(K,Rb)_2[Si_9W(CO)_4]_2^{6-} \cdot 6NH_3$ dimers are observed, resulting from the double cage coordination of A1. These dimers are connected by μ^2-ammonia bridged alkali metals to form a 2D network. The A@[2.2.2]crypt complexes separate these two-dimensional layers from each other.

Figure 4. Representation of the atomic distances from the single crystal X-Ray diffraction model, ZORA-D3(BJ)-B3LYP/ma-ZORA-def2-TZVP (Si, C, O), ZORA-D3(BJ)-B3LYP/Sarc-ZORA-TZVP (W) level and ZORA-D3(BJ)-PBE0/ma-ZORA-def2-TZVP (Si, C, O), ZORA-D3(BJ)-PBE0/Sarc-ZORA-TZVP (W) calculations on $[Si_9W(CO)_4]^{6-}$.[32,33,35–41]

Chemical Bonding

The complex anion $[Si_9W(CO)_4]^{6-}$ is structurally related to the tungsten pentacarbonylate $[W(CO)_5]^{2-}$, which from the point of view of organometallics can be described as an 18-valence electron cluster.[28] The configuration is achieved by five CO ligands, six electrons from the metal centre and two negative charges. One of the CO ligands here is replaced by a $[Si_9]^{4-}$ cluster as ligand. *Sevov et al.* stated that the $[Ge_{10}]^{2-}$ in the structure $[Ge_{10}Mn(CO)_4]^{3-}$ acts as a two-electron ligand *via* the coordination of a lone pair.[15] The corresponding molecular orbitals HOMO-3 ($[Si_9]^{4-}$) and LUMO ($[W(CO)_4]^{2-}$) support the description of $[Si_9]^{4-}$ as a two-electron donor ligand (Figure 3).

To reinforce the similarity, theoretical calculations on a ZORA-D3(BJ)-B3LYP/ma-ZORA-def2-TZVP (Si, C, O) ZORA-D3(BJ)-B3LYP/Sarc-ZORA-TZVP (W) level of theory were carried out for the anion $[Si_9W(CO)_4]^{6-}$.[32,33,35–41] The geometry optimized dimensions of the anion agree with the results of the X-Ray characterized compound and were confirmed as an energetic minimum by frequency analysis (Figure 4).
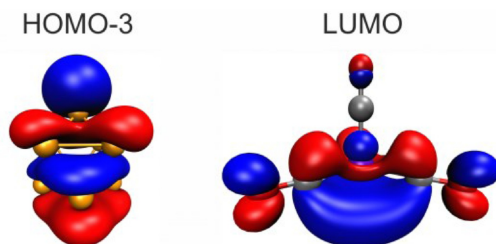
The {Si_9} unit of the calculated structure is described *via* a C_{4v}-symmetry with a d1/d2 ratio of 1.00 and a h/e ratio of 1.18. Compared to the calculated model, the strong distortion of the experimentally determined compound presumably is induced by the crystal packing effects. The converged W–Si distance is 2.684 Å and the silicon cage is coordinating with the apical atom which caps the square face.

Viewing the Laplacian of the electron density on the Si–W–(CO) plane and along the Si–W bond axis (Figure 5), it is strongly indicated that the Si lone pair is donating electrons to the W. Further evaluation of the bonding situation with a QTAIM analysis of the bond critical point (BCP) resulted in a positive ϱ, $\nabla^2\varrho$ and a negative virial potential energy density at the BCP. This can be, according to the criteria of *Bianchi et al.*, interpreted as a dative bond.[42,43]

Comparing the NPA and Bader charges of $[Si_9W(CO)_4]^{6-}$ (NPA: C/O = 0.222–0.367/−0.699−−0.718; Bader: C/O = 0.378–0.486/−1.311−−1.319) to a neutral CO fragment (NPA: C/O = 0.489/−0.489; Bader: C/O = 1.193/−1.193) the CO groups in the complex show higher negative charges compared to the neutral

Figure 3. Molecular orbitals HOMO-3 of $[Si_9]^{4-}$ and LUMO of $[W(CO)_4]^{2-}$. The molecular orbitals were calculated on a ZORA-D3(BJ)-B3LYP/ma-ZORA-def2-TZVP (Si, C, O), ZORA-D3(BJ)-B3LYP/Sarc-ZORA-TZVP (W) level of theory.[32–40]
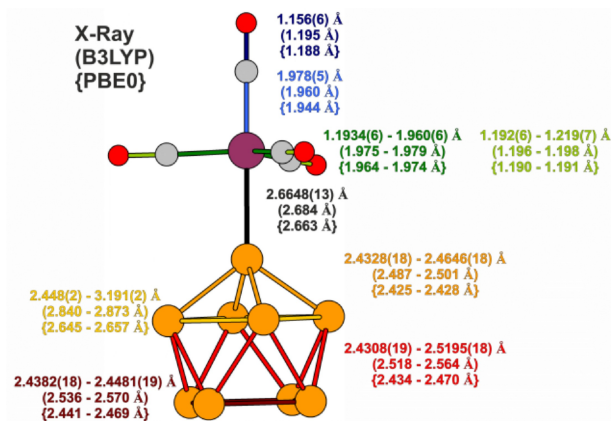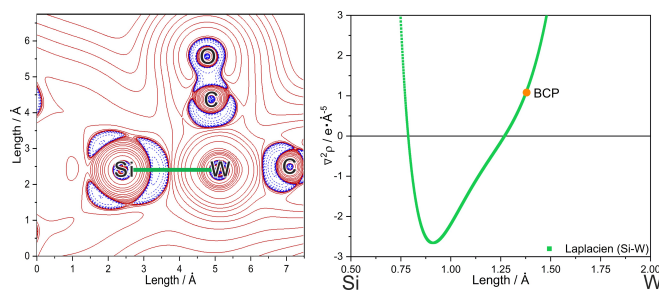

Figure 5. Contour line map showing the Laplacian of the electron density along the Si–W–C plane with positive values in red and negative values in blue and the Laplacian along the Si–W bond axis in green. The contour line map was plotted using Multiwfn.[44]

fragment.[34,43] Also, the delocalization index (DI) of the bound CO group is lower compared to the neutral fragment which indicates a weaker CO bonding. If the anion would be separated, the expected charges for the {Si$_9$} ligand would be 4− and 2− for the {W(CO)$_4$} (Figure 6). The NPA/Bader charges suggest an electron shift from the {Si$_9$} ligand towards the metal carbonylate since the overall charges are −3.586/−3.595 for {Si$_9$} and −2.414/−2.404 for {W(CO)$_4$}. More specifically the capped square plane of the {Si$_9$} antiprism shows a deficit of charge of 0.414 which is relocated mostly towards the W and partially towards the O atoms. This interpretation could be supported further by IR or Raman measurements, which were not successful until now because of the poor solubility of the compound and the lability of the solid ammoniate.

NMR Spectroscopic Studies

Preliminary NMR-Measurements of samples containing [W-(CO)$_4$(tmeda)], 99.2 % ^{29}Si-enriched K$_6$Rb$_6$Si$_{17}$ and [2.2.2]crypt in a molar ratio of 1 : 1 : 2 in liquid ammonia were carried out at 203 K. ^{183}W is the only naturally occurring isotope of tungsten with nuclear spin quantum number $I = \frac{1}{2}$ and a natural abundance of 14.3 % (All other natural isotopes have nuclear spin quantum number $I = 0$). While direct observation of ^{183}W-NMR is possible, it is usually not accessible with standard NMR hardware due to its very low resonance frequency (below ^{109}Ag). Surprisingly, alongside the known signal of [μ-HSi$_4$]$^{3−}$ we were able to detect an unprecedented ^{1}H-NMR signal at −4.796 ppm six months after sample preparation (Figure SI10).[24] It had exotic satellite integrals (Figure SI11), which were simulated and thus unambiguously assigned to originate from a ^{1}H-^{183}W coupling with a presumably ^1J-coupling constant of 53.3 Hz, in accordance with literature (Figure SI12).[45] Since this signal is not observed in samples containing only [W-(CO)$_4$(tmeda)] in liquid ammonia, it can be assumed, that K$_6$Rb$_6$Si$_{17}$ plays a vital role in its formation (Figure SI13). Unfortunately, unambiguous evidence for the presence of the
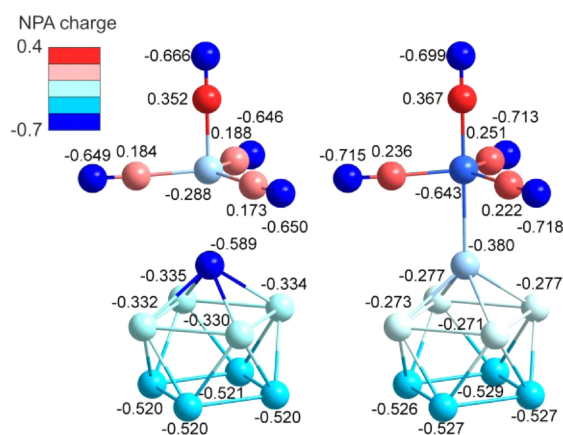
complex [(K,Rb)@([2.2.2]crypt)]$_2$(K,Rb)$_4$[Si$_9$W(CO)$_4$]·13.4 NH$_3$ in solution by means of direct observation of a ^{29}Si-signal with ^{183}W satellites could not be generated yet.

On the other hand, the presence of the new ^{1}H-signal corroborates the statement that [W(CO)$_4$(tmeda)] has labile ligands at the applied reaction conditions, while simultaneous observation of [μ-HSi$_4$]$^{3−}$ indicates that silicides are still present in solution and could react as potential ligands towards tungsten without decomposition.

Further investigations concerning the protonated tungsten species and attempts of direct detection of [(K,Rb)@-([2.2.2]crypt)]$_2$(K,Rb)$_4$[Si$_9$W(CO)$_4$]·13.4 NH$_3$ are in progress.

Conclusions

The use of the heteroleptic tmeda tungsten carbonyl complex [W(CO)$_4$(tmeda)] together with the nominal Zintl phase K$_6$Rb$_6$Si$_{17}$ in solution experiments in liquid ammonia allowed the crystallization of the compound [(K,Rb)@([2.2.2]crypt)]$_2$(K,Rb)$_4$ [Si$_9$W(CO)$_4$]·13.4 NH$_3$. The compound was analyzed *via* single crystal X-Ray diffraction and proved the presence of the pseudo pentagonal bipyramidal tungsten complex anion [Si$_9$W(CO)$_4$]$^{6−}$. The highly charged anion is stabilized by direct ion interactions of the four cations around the W−Si bond. The structure represents the first tungsten functionalized nonasilicide Zintl anion and only the sixth transition metal functionalized bare silicon cluster. Theoretical calculations suggest a dative Si−W bonding interaction is responsible for the formation of this new [Si$_9$W(CO)$_4$]$^{6−}$ complex anion.

Methods Section

All operations were conducted under argon atmosphere using standard glove box and Schlenk technique. Liquid ammonia was dried and stored over sodium cooled by an ethanol/dry ice bath dewar for at least 96 h.

Synthesis of K$_6$Rb$_6$Si$_{17}$ and K$_6$Rb$_6$^{29}Si$_{17}$ (99.2 % enriched): Potassium (766.1 mg, 19.59 mmol), rubidium (1674.7 mg, 19.59 mmol) and silicon (1559.2 mg, 55.16 mmol) were weighed, filled into a tantalum ampoule, welded shut and enclosed into a quartz glass ampoule. The ampoule was heated up to 1223 K at a rate of 50 K/h and after 2 h cooled to room temperature at a rate of 20 K/h.[46] K$_6$Rb$_6$^{29}Si$_{17}$ was synthesised according to the method described by *Streitferdt et al.*[25]

Synthesis of W(CO)$_4$(tmeda): The compound was synthesized *via* an adapted method reported by *King* and *Fronzaglia*.[47] The solvents used were degassed beforehand. In a two-neck flask a mixture of [W(CO)$_6$] (5 g, 14.2 mmol), tetramethylethylenediamine (5 mL, 39.0 mmol), 80 mL n-decane and a few mL *n*-hexane are refluxed for 27 h. The reaction mixture was left for crystallization at 253 K overnight. The solvent was removed, the crystals were washed three times with *n*-hexane and once with dichloromethane. ^{13}C NMR (400 MHz, CDCl$_3$): δ = 61.94 ppm (s, 2 C), δ = 57.73 ppm (s, 4 C).

Synthesis of [(K,Rb)@([2.2.2]crypt)]$_2$(K,Rb)$_4$[Si$_9$W(CO)$_4$]·13.4 NH$_3$: K$_6$Rb$_6$Si$_{17}$, W(CO)$_4$(tmeda) and [2.2.2]crypt were weighed into a flame-dried Schlenk vessel (1 : 1 : 1.5) and ammonia (10 mL) was

Figure 6. NPA charges of [Si$_9$]$^{4−}$, [W(CO)$_4$]$^{2−}$ and [Si$_9$W(CO)$_4$]$^{6−}$ calculated on a ZORA-D3(BJ)-B3LYP/ma-ZORA-def2-TZVP (Si, C, O), ZORA-D3(BJ)-B3LYP/Sarc-ZORA-TZVP (W) level of theory.[32–40]

condensed into the reaction vessel forming a brown-red solution. After storage for 12 weeks at 203 K, an abundance of dark red crystals could be observed and analyzed *via* X-ray single crystal diffraction.

X-ray diffraction studies: The compound was found to be highly moisture-, air- and temperature-sensitive. Due to these circumstances the crystals were transferred directly from the cooled Schlenk vessel into a nitrogen stream cooled perfluoroether oil. Suitable crystals were picked up using a MiTeGen loop and transported to the diffractometer using liquid nitrogen for cooling. The diffractometer used was a Rigaku Synergy DW with a photon Jet-DW VHF Cu X-ray source and a HyPix Arc 150° detector. Data collection was performed at a temperature of 123 K. For data reduction and absorption correction the software *CrysAlisPro* (version 171.43.36a[48]) was used. The structure solution (*ShelXT*[49]) and refinement (*ShelXL*[50]) was performed in Olex^2 1.5 alpha.[51] The figures were created in Diamond 4 using displacement ellipsoids at 50% probability level.[52]

All atoms (except H) could be located in the electron density map. H atoms of the ammonia molecules of solvation were constructed using a riding restraint (Afix 137). The H atoms of the ammonia molecule N15 could not be constructed in a meaningful way. The occupancy of the ammonia molecule N4 was refined to a value of 0.369(17).

Crystal data for [(K,Rb)@([2.2.2]crypt)]$_2$(K,Rb)$_4$[Si$_9$W(CO)$_4$]·13.4 NH$_3$: $M_r = 1870.72$, space group $P\bar{1}$, $\mu = 7.791$ mm^{-1}, $\rho_{calc} = 1.523$ g m^{-3}, $a = 11.48390(10)$ Å, $b = 19.7383(2)$ Å, $c = 19.8983(2)$ Å, $\alpha = 112.5760(10)°$, $\beta = 97.4210(10)°$, $\gamma = 95.3760(10)°$, $V = 4079.01(7)$ Å^3, $Z = 2$, 72249 measured reflections, 16465 independent reflections, $R_{int} = 0.0555$, $R_1 = 0.0482/wR_2 = 0.1263$ (I ≥ 2σ(I)), $R_1 = 0.0596/wR_2 = 0.1325$ (all data), GOOF = 1.055, $\Delta\rho_{max} = 1.44$ Å^{-3}, $\Delta\rho_{min} = -1.61$ Å^{-3}.

Crystallographic data for the structure has been deposited in the Cambridge Crystallographic Data Centre, CCDC, 12 Union Road, Cambridge CB21EZ, UK. Copies of the data can be obtained free of charge on quoting the depository number CCDC-2260797 (Fax: +44-1223-336-033; E-Mail: deposit@ccdc.cam.ac.uk, http://www.ccdc.cam.ac.uk).

Sample preparation for NMR studies: K$_6$Rb$_6$^{29}Si$_{17}$ (99.2% enriched, 6.3 mg, 0.005 mmol), [W(CO)$_4$(tmeda)] (2.1 mg, 0.005 mmol) and [2.2.2]crypt (3.8 mg, 0.010 mmol) were weighed into a flame-dried heavy wall precision NMR tube (Pyrex) under argon atmosphere. Ammonia was condensed into the tube, yielding a light red solution and it was sealed shut under ammonia atmosphere. The sample was stored at 195 K until NMR examination.

NMR studies: NMR-Spectroscopic measurements in liquid NH$_3$ were recorded on a Bruker Avance III 600 MHz spectrometer equipped with a 5 mm TBI–P probe (^{1}H, ^{31}P, X) with z-gradient without using ^{2}H-lock. A N$_2$ evaporator unit was used for measurements at 203 K. ^{1}H-NMR measurements without presaturation were performed using a standard Bruker pulse program (zg) with 32 scans, relaxation delay of 3 seconds and acquisition time of 1.81 seconds. If not noted otherwise, optimized ^{1}H-NMR measurements with presaturation of the ammonia signal were performed using a standard Bruker pulse program (zggppr) with 512 scans, relaxation delay of 3 seconds and acquisition time of 2.5 seconds. Data were processed with the Bruker software TopSpin 4.2.0 using the parameters SI = 131072, WDW = "EM", LB = 2 (Hz). Baselines of integrated spectra were corrected using cubic splines ("sab" command in TopSpin. ^{1}H-NMR chemical shifts are reported relative to center of the solvent signal of NH$_3$ at 1.21 ppm.

Quantum chemical calculations: The calculations on [Si$_9$W(CO)$_4$]$^{6-}$, [Si$_9$]$^{4-}$ and [W(CO)$_4$]$^{2-}$ were performed using Orca 5.0.3 employing a ZORA-D3(BJ)-B3LYP/ma-ZORA-def2-TZVP (Si, C, O), ZORA-D3(BJ)-B3LYP/Sarc-ZORA-TZVP (W) level of theory using a CPCM model of ammonia.[32,35–40] For [Si$_9$W(CO)$_4$]$^{6-}$ also a ZORA-D3(BJ)-PBE0/ma-ZORA-def2-TZVP (Si, C, O), ZORA-D3(BJ)-PBE0/Sarc-ZORA-TZVP (W) level of theory (CPCM: ammonia) calculation was performed.[41] The NPA charges were calculated using NBO 7.0.9[34] and the QTAIM charges using AIMAII.[43] The Laplacian was plotted using Multiwfn[44] and the line graph was made in Origin 9.9.0.225.[53] The molecular orbitals were plotted in orca plot and visualized using VMD.[38,54]

Acknowledgements

Conflict of Interest

The authors declare no conflict of interest.

Data Availability Statement

The data that support the findings of this study are available in the supplementary material of this article.

[1] A. C. Joannis, *C. R. Hebd. Seances Acad. Sci.* **1891**, *113*, 795–798.

[2] M. Beekman, S. Kauzlarich, L. Doherty, G. Nolas, *Materials* **2019**, *12*, 1139.

[3] L.-A. Jantke, A. J. Karttunen, T. F. Fässler, *Z. Anorg. Allg. Chem.* **2023**, *649*, 1–9.

[4] a) S. C. Sevov, J. M. Goicoechea, *Organometallics* **2006**, *25*, 5678–5692; b) Y. Heider, D. Scheschkewitz, *Chem. Rev.* **2021**, *121*, 9674–9718.

[5] R. J. Wilson, N. Lichtenberger, B. Weinert, S. Dehnen, *Chem. Rev.* **2019**, *119*, 8506–8554.

[6] C. Liu, Z.-M. Sun, *Coord. Chem. Rev.* **2019**, *382*, 32–56.

[7] S. Scharfe, F. Kraus, S. Stegmaier, A. Schier, T. F. Fässler, *Angew. Chem. Int. Ed.* **2011**, *50*, 3630–3670.

[8] a) B. W. Eichhorn, R. C. Haushalter, W. T. Pennington, *J. Am. Chem. Soc.* **1988**, *110*, 8704–8706; b) B. W. Eichhorn, R. C. Haushalter, *J. Chem. Soc. Chem. Commun.* **1990**, 937–938; c) J. Campbell, H. P. A. Mercier, H. Franke, D. P. Santry, D. A. Dixon, G. J. Schrobilgen, *Inorg. Chem.* **2002**, *41*, 86–107.

[9] B. Kesanli, J. Fettinger, B. Eichhorn, *Chem. Eur. J.* **2001**, *7*, 5277–5285.

[10] L. Yong, S. D. Hoffmann, T. F. Fässler, *Eur. J. Inorg. Chem.* **2005**, 3663–3669.

[11] a) C. Schenk, A. Schnepf, *Chem. Commun.* **2009**, 3208–3210; b) F. Henke, C. Schenk, A. Schnepf, *Dalton Trans.* **2011**, *40*, 6704–6710.

[12] a) R. S. P. Turbervill, J. M. Goicoechea, *Chem. Rev.* **2014**, *114*, 10807–10828; b) K. Beuthert, B. Peerless, S. Dehnen, *Commun. Chem.* **2023**, *6*, 109; c) S. Charles, B. W. Eichhorn, A. L. Rheingold, S. G. Bott, *J. Am. Chem. Soc.* **1994**, *116*, 8077–8086; d) L. Qiao, D. Chen, J. Zhu, A. Muñoz-Castro, Z.-M. Sun, *Chem. Commun.* **2021**, *57*, 3656–3659; e) L. Xu, A. Ugrinov, S. C. Sevov, *J. Am. Chem. Soc.* **2001**, *123*, 4091–4092; f) Y.-H. Xu, N. V. Tkachenko, I. A. Popov, L. Qiao, A. Muñoz-Castro, A. I. Boldyrev, Z.-M. Sun, *Nat. Commun.* **2021**, *12*, 4465.

[13] L. Wang, Y. Wang, Z. Li, H. Ruan, L. Xu, *Dalton Trans.* **2017**, *46*, 6839–6842.

[14] a) P. Kircher, G. Huttner, K. Heinze, G. Renner, *Angew. Chem. Int. Ed.* **1998**, *37*, 1664–1666; b) G. Renner, P. Kircher, G. Huttner, P. Rutsch, K. Heinze, *Eur. J. Inorg. Chem.* **2001**, *2001*, 973–980.

[15] D. Rios, S. C. Sevov, *Inorg. Chem.* **2010**, *49*, 6396–6398.

[16] Y.-S. Huang, D. Chen, J. Zhu, Z. M. Sun, *Chin. Chem. Lett.* **2022**, *33*, 2139–2142.

[17] B. Zhou, J. M. Goicoechea, *Chem. Eur. J.* **2010**, *16*, 11145–11150.

[18] C. Liu, L.-J. Li, Q.-J. Pan, Z.-M. Sun, *Chem. Commun.* **2017**, *53*, 6315–6318.

[19] a) E. N. Esenturk, J. Fettinger, B. Eichhorn, *Polyhedron* **2006**, 521–529; b) B. Kesanli, J. Fettinger, D. R. Gardner, B. Eichhorn, *J. Am. Chem. Soc.* **2002**, *124*, 4779–4786; c) C. Liu, L.-J. Li, X. Jin, J. E. McGrady, Z.-M. Sun, *Inorg. Chem.* **2018**, *57*, 3025–3034; d) C. Lorenz, *Dissertation, Univ. Regensburg* **2019**

[20] J. M. Goicoechea, S. C. Sevov, *Organometallics* **2006**, *25*, 4530–4536.

[21] S. Gärtner, M. Hamberger, N. Korber, *Crystals* **2015**, *5*, 275–282.

[22] a) M. Waibel, F. Kraus, S. Scharfe, B. Wahl, T. F. Fassler, *Angew. Chem. Int. Ed.* **2010**, *49*, 6611–6615; b) S. M. Tiefenthaler, V. Streitferdt, J. Baumann, S. Gaertner, R. M. Gschwind, N. Korber, *Z. Anorg. Allg. Chem.* **2020**, *646*, 1595–1602; c) F. S. Geitner, T. F. Fässler, *Chem. Commun.* **2017**, *53*, 12974–12977; d) S. Joseph, M. Hamberger, F. Mutzbauer, O. Hartl, M. Meier, N. Korber, *Angew. Chem. Int. Ed.* **2009**, *48*, 8770–8772.

[23] a) C. Lorenz, F. Hastreiter, J. Hioe, N. Lokesh, S. Gärtner, N. Korber, R. M. Gschwind, *Angew. Chem. Int. Ed.* **2018**, *57*, 12956–12960; b) L. J. Schiegerl, A. J. Karttunen, J. Tillmann, S. Geier, G. Raudaschl-Sieber, M. Waibel, T. F. Fässler, *Angew. Chem. Int. Ed.* **2018**, *130*, 13132–13137.

[24] F. Hastreiter, C. Lorenz, J. Hioe, S. Gärtner, N. Lokesh, N. Korber, R. Gschwind, *Angew. Chem.* **2019**, *131*, 3165–3169.

[25] V. Streitferdt, S. M. Tiefenthaler, I. G. Shenderovich, S. Gärtner, N. Korber, R. M. Gschwind, *Eur. J. Inorg. Chem.* **2021**, *36*, 3684–3690.

[26] S. Gärtner, N. Korber, in: – *Comprehensive Inorganic Chemistry II: From Elements to Applications*, 2nd ed. (Eds.: J. Reedijk, J. Poeppelmeier), Elsevier Ltd., Amsterdam **2013**, pp. 251–267

[27] S. Joseph, C. Suchentrunk, F. Kraus, N. Korber, *Eur. J. Inorg. Chem.* **2009**, *31*, 4641–4647.

[28] J. M. Maher, R. P. Beatty, N. J. Cooper, *Organometallics* **1985**, *4*, 1354–1361.

[29] G. Pei, C.-C. Shu, L. Mengyang, Z.-M. Sun, T. Yang, *Phys. Chem. Chem. Phys.* **2021**, 18640–18646.

[30] a) S. Schmitzer, U. Weis, H. Kaeb, W. Buchner, W. Malisch, T. Polzer, U. Posset, W. Kiefer, *Inorg. Chem.* **1993**, *32*, 303–309; b) T. S. Koloski, D. C. Pestana, P. J. Carroll, D. H. Berry, *Organometallics* **1994**, *13*, 489–499.

[31] J. E. Ellis, G. P. Hagen, *J. Am. Chem. Soc.* **1974**, *96*, 7825–7826.

[32] A. D. Becke, *J. Chem. Phys.* **1993**, *98*, 1372-1377.

[33] A. D. Becke, *Phys. Rev.* **1988**, *A38*, 3098.

[34] E. D. Glendening, Badenhoop, J, K., A. E. Reed, J. E. Carpenter, J. A. Bohmann, C. M. Morales, P. Karafiloglou, C. R. Landis, F. Weinhold, *NBO 7.0*, Theoretical Chemistry Institute, University of Wisconsin, Madison **2018**

[35] S. Grimme, S. Ehrlich, L. Goerigk, *J. Comput. Chem.* **2011**, *32*, 1456–1465.

[36] S. Grimme, J. Antony, S. Ehrlich, H. Krieg, *J. Chem. Phys.* **2010**, *132*, 154104.

[37] C. Lee, W. Yang, R. G. Parr, *Phys. Rev.* **1988**, *B37*, 785–789.

[38] F. Neese, *WIREs Comput. Mol. Sci.* **2022**, *12*, 1–15.

[39] D. A. Pantazis, X. Y. Chen, C. R. Landis, F. Neese, *J. Chem. Theory Comput.* **2008**, *4*, 908.

[40] F. Weigend, *Phys. Chem. Chem. Phys.* **2006**, *8*, 1057.

[41] C. Adamo, V. Barone, *J. Chem. Phys.* **1999**, *110*, 6158–6170.

[42] a) R. Bianchi, G. Gervasio, D. Marabello, *Inorg. Chem.* **2000**, *39*, 2360–2366; b) C. Lepetit, P. Fau, K. Fajerwerg, M. L. Kahn, B. Silvi, *Coord. Chem. Rev.* **2017**, *345*, 150–181; c) R. F. W. Bader, *Monatsh. Chem.* **2005**, *136*, 819–854.

[43] T. A. Keith, *AIMAll*, TK Gristmill Software, Overland Park KS, USA **2019**.

[44] T. Lu, F. Chen, *J. Comput. Chem.* **2012**, *33*, 580–592.

[45] T. Vielhaber, C. Heizinger, C. Topf, *J. Catal.* **2021**, *404*, 451–461.

[46] a) C. Hoch, M. Wendorff, C. Roehr, *J. Alloys Compd.* **2003**, *361*, 206–221; b) S. V. Sevov, E. Todorov, V. Quéneau, *J. Am. Chem. Soc.* **1998**, *120*, 3263–3264.

[47] R. B. King, A. Fronzaglia, *Inorg. Chem.* **1966**, *5*, 1837–1846.

[48] *CrysAlisPro*, Diffraction Rigaku Oxford **2017**.

[49] G. M. Sheldrick, *Acta Crystallogr. Sect. A* **2015**, 3–8.

[50] G. M. Sheldrick, *Acta Crystallogr. Sect. C* **2015**, 3–8.

[51] a) O. V. Dolomanov, L. J. Bourhis, R. J. Gildea, J. A. K. Howard, H. Puschmann, *J. Appl. Crystallogr.* **2009**, *42*, 339–341; b) L. J. Bourhis, O. V. Dolomanov, R. J. Gildea, J. A. K. Howard, H. Puschmann, *Acta Crystallogr. Sect. A* **2015**, *71*, 59–75.

[52] K. Brandenburg, *Diamond*, Version 4.6.8, Crystal Impact GbR, Bonn, Germany **2022**.

[53] *Origin*, OriginLab Corporation, Northhampton, MA, USA.

[54] W. Humphrey, A. Dalke, K. Schulten, *J. Mol. Graphics* **1996**, *14*, 33–38.

RESEARCH ARTICLE
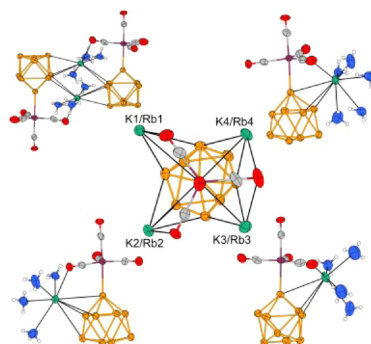
P. A. Braun, F. F. Westermair,
Prof. Dr. R. M. Gschwind, Prof. Dr. N.
Korber*

1 – 7

[(K,Rb)@([2.2.2]crypt)]$_2$(K,Rb)$_4$[Si$_9$W-(CO)$_4$]·13.4 NH$_3$ – The First Tungsten Functionalized Silicon Zintl Cluster